Author/s:
Chirico, GB;Grayson, RB;Western, AW

Title:
On the computation of the quasi-dynamic wetness index with multiple-flow-direction algorithms

Date:
2003-01-01

Citation:
Chirico, G. B., Grayson, R. B. & Western, A. W. (2003). On the computation of the quasi-dynamic wetness index with multiple-flow-direction algorithms. Water Resources Research, 39 (5), pp.TNN11-TNN17. https://doi.org/10.1029/2002WR001754.

Persistent Link:
https://hdl.handle.net/11343/297418

WATER RESOURCES RESEARCH, VOL. 39, NO. 5, 1115, doi:10.1029/2002WR001754, 2003

On the computation of the quasi-dynamic wetness index with multiple-flow-direction algorithms

Giovanni Battista Chirico,[1,2] Rodger B. Grayson, and Andrew W. Western

Centre for Environmental Applied Hydrology and Cooperative Research Centre for Catchment Hydrology, Department of Civil and Environmental Engineering, University of Melbourne, Victoria, Australia

Received 3 October 2002; revised 18 February 2003; accepted 5 March 2003; published 6 May 2003.

[1] The quasi-dynamic wetness index, in its original development, was computed by calculating the travel time along all the possible upslope flow paths on a contour-based terrain network. In more recent applications the same approach has been extended to gridded digital elevation models with single-flow-direction algorithms. Multiple-flow-direction algorithms, although more effective in representing flow paths, have not been used because they are not practicable with the established methodology. We propose an alternative method for computing the quasi-dynamic wetness index based on the numerical integration of the linear-kinematic wave equation. This method can be applied to any of the terrain-based flow-direction algorithms currently published. The method is robust and efficient. *INDEX TERMS:* 1815 Hydrology: Erosion and sedimentation; 1824 Hydrology: Geomorphology (1625); 1860 Hydrology: Runoff and streamflow; 1866 Hydrology: Soil moisture; *KEYWORDS:* quasi-dynamic wetness index, topographic wetness indices, terrain analysis, digital terrain model, kinematic flow

Citation: Chirico, G. B., R. B. Grayson, and A. W. Western, On the computation of the quasi-dynamic wetness index with multiple-flow-direction algorithms, *Water Resour. Res.*, *39*(5), 1115, doi:10.1029/2002WR001754, 2003.

1. Introduction

[2] Topographic wetness indices are largely used as similarity parameters for estimating the spatial distribution of soil moisture and runoff source areas. Traditional topographic wetness indices [*Beven and Kirkby*, 1979; *O'Loughlin*, 1981; *Ambroise et al.*, 1996] assume the specific upslope area as a surrogate for the local lateral discharge rate with the following underlying hypotheses: (1) uniform upslope recharge rate; (2) equilibrium condition of the upslope catchment response (steady state assumption); and (3) lateral flow parallel to the surface slope and therefore unit contour length equivalent to the unit flow width. The steady state assumption has been recognized as being the most limiting hypothesis, particularly in nonhumid areas, when the upslope catchment is far from being in equilibrium condition and only a limited portion is effectively contributing to the lateral discharge [*Jones*, 1986; *Barling et al.*, 1994; *Beven*, 1997; *Piñol et al.*, 1997; *Beven and Freer*, 2001].

[3] *Barling et al.* [1994] proposed the quasi-dynamic wetness index (QDWI) for the assessment of the soil moisture distribution, based on an effective contributing area accounting for the timing of the lateral soil moisture distribution. The QDWI is conceptually analogous to many traditional rational methods for assessing the flow peak, derived by applying rectangular hyetographs as design effective hyetographs and a linear model for simulating the catchment response [*Schaake et al.*, 1967]. The QDWI represents the wetness condition associated with the peak flow response produced by a uniform and constant upslope recharge rate of given duration, under the hypothesis of kinematic lateral flow routing, with time-independent patterns of lateral celerity. The peak response to rectangular hyetographs of different durations d is synthesized by the specific time-area curve $a(d)$. Curve $a(d)$ is the upslope plane area per unit flow width, located within a distance such that the flow can travel in a time equal to or less than d. It is also equal to the lateral flow per unit width due to a constant and uniform unit upslope vertical recharge after a time interval equal to d [*Clark*, 1945]. A generic formulation of the QDWI for a given duration d and recharge r [L/T] is

$$QDWI(r,d) = \frac{r \cdot a(d)}{c \cdot S} \quad (1)$$

where c [L/T] is the local lateral celerity and S [L] is the "effective" saturated soil moisture capacity.

[4] The assumption of constant lateral flow celerity, i.e., independent from the local wetness conditions, is a traditional modeling approach for runoff routing [e.g., *Beven et al.*, 1995]. However, it is not always appropriate for predicting lateral soil moisture distribution. *Barling et al.* [1994] applied the QDWI to predict the observed lateral soil moisture distribution in Wagga Wagga (Australia), an area characterized by shallow topsoil above a bottom horizon of low hydraulic conductivity. Assuming that the lateral distribution of soil moisture was primarily controlled by subsurface flow in a saturated zone of the topsoil, and are estimated with the following relations [*Barling et al.*, 1994]:

$$c = \frac{K_S \sin\vartheta}{\eta} \quad (2)$$

$$S = D\eta \quad (3)$$

[1]Also at Institut für Hydraulik, Gewässerkunde und Wasserwirtschaft, Technische Universität Wien, Vienna, Austria.

[2]Now at Department of Agricultural Engineering, University of Naples Federico II, Portici, Italy.

0043-1397/03/2002WR001754

K_S is the saturated hydraulic conductivity; D is the depth (orthogonal to the slope angle ϑ) of the topsoil within which lateral saturated subsurface flow develops, effectively contributing to lateral soil moisture distribution; η is the "effective" porosity, equal to the difference between soil apparent porosity and the initial soil wetness conditions. *Barling et al.* [1994] set the initial soil moisture equal to the field capacity, with the hypothesis that vertically infiltrating volumes rapidly redistribute and generate lateral subsurface flow, and they assumed η and K_S vertically uniform, such that the celerity of the subsurface flow is independent of the local wetness conditions. These assumptions are not realistic if lateral soil moisture distribution occurs within deep and vertically heterogeneous soils, but are reasonable where there is a shallow confining layer.

[5] The advantage of assuming constant lateral celerity resides in the possibility of synthesizing the topographical effects on the timing of lateral soil moisture distribution with a single parameter $a(d)$, independent from the actual recharge rate, to be used in a simple wetness index. If the hypothesis of constant celerity is relaxed, the patterns of wetness condition can be assessed only by routing the lateral flow for each design recharge rate over the entire element network, as is done in fully distributed models. A compromise is represented by some recent model developments, such as Dynamic TOPMODEL [*Beven and Freer*, 2001]. This approach restricts the lateral flow routing among a few units, representing classes of elements that are identified as having similar hydrological behavior on the basis of stationary properties. However, this still requires dynamic computation (as, of course, do fully distributed models). The need for any dynamic computation undermines the essential interest in index-style approaches, namely, that key effects of spatial organization can be captured by a single index.

[6] Since *Barling et al.* [1994], the QDWI has been applied in a few cases, related mainly to landslide mapping [e.g., *Duan and Grant*, 2000; *Chirico et al.*, 2001; *Gritzner et al.*, 2001; *Borga et al.*, 2002]. *Chirico et al.* [2001] and *Borga et al.* [2002] coupled the QDWI with the intensity-duration-frequency curves to identify the design recharge rate and duration of equation (1), analogous to what is done for estimating the peak flow with rational formulae [e.g., *Rossi and Villani*, 1994]. *Fried et al.* [2000] extended the QDWI concept to the stream power index, for assessing the sediment transport to the riparian zone.

[7] Patterns of $a(d)$ have been computed on element networks, consisting of a discrete representation of the terrain in elemental units, with defined patterns of lateral flow direction, distribution, and celerity [*Moore et al.*, 1991; *Barling et al.*, 1994]. Currently implemented methods follow a geometrical approach, consisting of accumulating the areas along the upslope flow paths that can be covered within a travel time less than or equal to d. *Barling et al.* [1994] first used this method on a contour-based element network. The same method has been then extended to gridded digital elevation models (DEMs) with single-flow-direction algorithms [*Wilson and Gallant*, 2000; *Borga et al.*, 2002]. The method has not been applied to gridded DEMs with multiple-flow-direction algorithms, although these have been shown to be better representations of surface flow paths than the single-flow-direction algorithms [*Tarboton*, 1997]. The reason is that the geometrical approach is not practicable with multiple-flow-direction algorithms, due to the extremely high number of alternative upslope flow paths generated by these algorithms [*Wilson and Gallant*, 2000]. In this technical note we suggest a new method that can handle any kind of flow-direction algorithm. It is more computationally efficient than the geometrical approach and can be used to produce QDWI patterns based on multiple-flow-direction algorithms. We first outline a generic representation of the flow path patterns on a discrete representation of the terrain. Then we present the method and show its robustness and efficiency with a numerical example.

2. General Representation of an Element Network

[8] An element network is an ordered set of connected plane elements. The spatial location of each element is generally identified by the spatial coordinate of the element center. The width of the lateral flow across the element is assumed to vary linearly from upslope to downslope in contour-based element networks, while it is assumed constant in grid-based element networks [*Gallant and Wilson*, 2000]. Therefore, in the most general case, the plan geometry of the element and the flow is characterized by the element area, the downslope width, and the element length. The connectivity defines for each element i, the downslope elements $j(i)$ and the proportion $p_i(j)$ of the outgoing lateral fluxes allocated to each of the downslope elements $j(i)$. The proportion factors $p_i(j)$ are subjected to the condition

$$\sum_j p_i(j) \leq 1. \tag{4}$$

The sum above is less than 1 when the element i allocates part of the outgoing flow across the boundary of the study area or in an internal pit. It is worth noting that it is not necessary for the boundary of the study area to coincide with the boundary of a specific catchment; rather it need only include all the area upslope of the study area that contributes flow for the duration of interest. Once the element connectivity is defined, elements can be ordered to form a cascade of one-dimensional flow paths, according to a sequence integer number, such that the generic element i does not have any element in the upslope area with element number larger than i.

3. Numerical Method for Computing the Quasi-Dynamic Wetness Index

[9] Given its definition, $a(d)$ patterns can be computed by integrating the kinematic flow on an element network with a uniform vertical recharge rate r [L/T] for a duration up to d. Each element i of the network can be identified as a single channel of width $w_i(s)$ linearly varying between the upslope (s = 0) and the downlsope ($s = l_i$) extremes. The kinematic flow equation along the element slope per unit vertical recharge rate is

$$\frac{\partial Q_i}{\partial s} + \frac{1}{c_i}\frac{\partial Q_i}{\partial t} = w_i(s) r \cos\vartheta_i \tag{5}$$

where c_i is the element celerity, $Q_i(s, t)$ is the discharge, and $r\cos\vartheta_i$ represents the uniform recharge rate per unit element area along the slope ϑ_i. The ratio $\tau_i = l_i/c_i$ represents the characteristic timescale of each element. The initial conditions are set uniformly equal to zero when computing the QDWI [*Barling et al.*, 1994], while the upslope condition is given by the sum of the discharge $Q_j(t) = Q_j(l_j, t)$ from the upslope elements:

$$\begin{aligned} Q(s, t = 0) &= 0 \\ Q(s = 0, t) &= \sum_j Q_j(t) p_j(i) \end{aligned} \tag{6}$$

The value of $Q_j(t)$ is known if the kinematic wave is integrated for each element following the order of the element sequence number.

[10] For a generic duration d, the effective contributing area $a_i(d)$ is given by [*Barling et al.*, 1994]

$$a_i(d) = \frac{Q_i(d)}{r \cdot w_i(l_i)} \tag{7}$$

The system of equations (5) and (6) can be resolved numerically. There are not any practical limitations in the choice of spatial and temporal discretization with respect to obtaining stable solutions with limited numerical dispersion (see below). In order to compute the whole range of possible $a(d)$ patterns, the numerical integration has to be run only once for t up to the time of concentration, i.e., the longest flow path travel time in the study area. Moreover, once $a(d)$ patterns are known for a given distribution of the lateral flow celerity c, it is easy to derive the $a^1(d)$ patterns for any celerity patterns c^1 equal to the original pattern c scaled by a constant value λ, such as $c^1 = \lambda c$. In fact, in this case $a^1(d)$ can be simply obtained by scaling $a(d)$ in time by the same constant value λ: $a^1(d) = a(d/\lambda)$. This property is highly relevant in practical applications, because lateral flow celerity is often assumed to be proportional to the tangent or the sine of the local slope angle, with a proportionality factor defined by parameters, such as K_S and η in equation (2), uniform across all the study area. These parameters depend on the nature of the lateral flow to be studied and are generally defined by calibration and/or by field measurements [e.g., *Fried et al.*, 2000; *Borga et al.*, 2002].

[11] Many distributed hydrological models implement the kinematic wave for routing lateral flow with various types of spatial discretization of the catchment area [e.g., *Grayson et al.*, 1992; *Smith et al.*, 1995]. The adopted finite difference schemes are all special cases of the following generalized finite difference scheme, examined by *Smith* [1980]:

$$\frac{\left[\beta\left(Q_i^{(4)} - Q_i^{(2)}\right) + (1-\beta)\left(Q_i^{(3)} - Q_i^{(1)}\right)\right]}{\Delta s} + \frac{\left[\alpha\left(Q_i^{(2)} - Q_i^{(1)}\right) + (1-\alpha)\left(Q_i^{(4)} - Q_i^{(3)}\right)\right]}{c_i \Delta t} = \overline{w}_i r \cos\vartheta_i \tag{8}$$

where Q_i superscripts 1 and 3 refer to the time t at the positions s and $s + \Delta S$, respectively; superscripts 2 and 4 refer to the time $t + \Delta t$ at positions s and $s + \Delta S$, respectively; $\bar{w}_i$ is the average flow width between s and $s + \Delta S$; and α and β are weighting factors in the space and time directions, respectively. A stable solution can be obtained for [*Smith*, 1980]:

$$\frac{\alpha}{\beta} \le C_r \le \frac{1-\alpha}{1-\beta}; \qquad C_r = c_i \frac{\Delta t}{\Delta s} \tag{9}$$

where C_r is the Courant number. *Smith* [1980] showed that the scheme has a second-order accuracy for $\alpha = \beta = 0.5$ and that the first-order truncation errors in s and t increase independently as α and β depart from 0.5. It is important to note that in most practical circumstances the celerity is set proportional to the slope, which varies over more than 1 order of magnitude. Therefore, for a given Δt, Δs should be set for each element in order to satisfy the condition in equation (9). A generally practicable approach is to set Δt equal to a fraction f of the minimum element characteristic time τ_{min} to ensure limited truncation error in time, while varying the space-step Δs from element to element, as a submultiple of the element length, $\Delta s = l_i/n_i$, so that the condition of equation (9) is satisfied. The parameters α, β, and f are chosen so that an integer n_i can be always found within the following limits:

$$\frac{\tau_i}{f \cdot \tau_{min}} \frac{\alpha}{\beta} \le n_i \le \frac{\tau_i}{f \cdot \tau_{min}} \frac{1-\alpha}{1-\beta} \tag{10}$$

A value of $\alpha = 0.5$ is to be preferred to avoid first-order truncation errors in space and significant errors in continuity [*Smith*, 1980]. For $\alpha = 0.5$, an integer within the range of equation (10) always exists if

$$\begin{aligned} &\beta \ge 2/3 && f \ge 0.75 \\ &\beta \ge \left[\sqrt{(1+f^2)} - (1-f)\right]/2f && f \le 0.75 \end{aligned} \tag{11}$$

In general, more than one integer number n_i can occur within the limit of equation (10). The smallest integer number n_i is to be preferred, as it implies coarser spatial discretization and therefore less computational effort, without a significant increase in truncation errors. Larger n_i values, i.e., finer spatial resolution, do not increase significantly the computational accuracy, as this only affects the second-order truncation errors in space. The first-order truncation errors in time are more important. These can be reduced by choosing smaller f values and, β as a consequence, as close as possible to 0.5, given the condition in equation (11). The parameter f should be chosen accounting for the level of accuracy needed within the range of durations of interest, considering that smaller f leads to larger computational effort and that significant truncation errors only occur when the kinematic wave is characterized by steep fronts. Steep fronts are generally associated with areas of high planar and profile curvature (e.g., channel heads) for durations less than the upslope concentration time.

4. Numerical Example

[12] In this section we present a test of the numerical approach illustrated above. The $a(d)$ patterns computed with the numerical approach are compared with those computed with the traditional geometrical method. The test is performed on a grid with flow paths defined by both the single-flow-direction algorithm D8 [*O'Callaghan and Mark*, 1984] and the multiple-flow-direction algorithm D∞ [*Tar-*

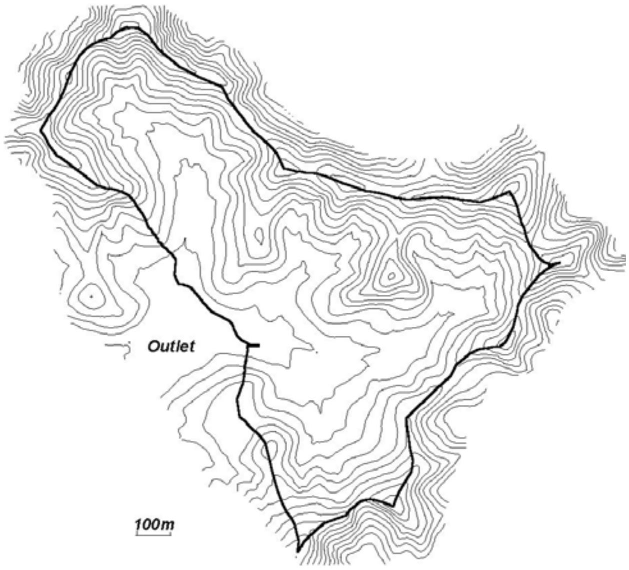

Figure 1. Contour map and boundary of the sample area. Contour spacing is 5 m.

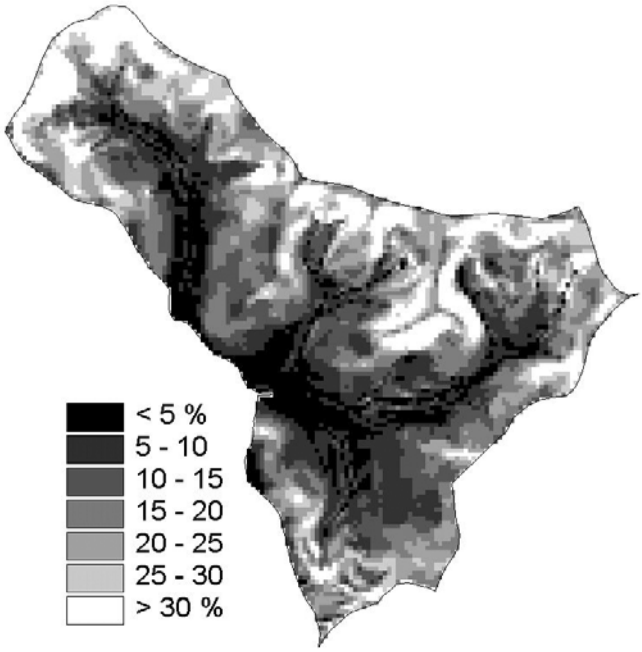

Figure 2. Slope map computed with the D8 algorithm on a 10-m-grid digital elevation model.

boton, 1997]. The sample area is the 1 km^2 Satellite Station catchment, in the north island of New Zealand [*Woods et al.*, 2001] (Figure 1). This area is chosen because its topography provides a strong test for the numerical scheme outlined above. The ridge area is composed of 13 peaks along the boundary and two internal peaks. Valley areas are crossed by four main channels. Slope and aspect vary considerably within short distances. Slope ranges from 1% to more than 30%, while landscape aspect covers a 360° range. The sample area is discretized in an element network of 8857 pixels derived from a 10-m-grid DEM. Figure 2 shows the topographic slope computed with the D8 algorithm. The pattern of lateral celerity is set equal to the sine of the slope angle, $c_i = \sin\vartheta_i$ m/s. This is a representative pattern, and as explained above, it is commonly used in practical applications to define the scaling of celerity.

[13] For the computation of $a(d)$ using the numerical method and the geometrical methods, Fortran codes have been compiled and executed on a desktop computer with a 2.4-GHz CPU, under the Windows® operating system. The algorithm used for the geometrical method is similar to that implemented in DYNWET [*Barling et al.*, 1994; *Wilson and Gallant*, 2000]. Figure 3 shows the pattern of the upslope time of concentration computed with the geometrical approach using the D8 flow path pattern. Average time of concentration of the hillslopes is about 1000 s, while the maximum time of concentration in the valley areas is 46,000 s. The application of the geometrical approach on the D∞ flow path pattern proved impracticable for durations above 1500 s. The number of alternative upslope flow paths rapidly increases as the duration increases. For example, the maximum number of alternative flow paths associated with one pixel increases from 69,533 to 571,399 as the duration increases from 1000 to 1500 s. For a duration of 2000 s, the program execution was stopped after 4 hours without having found the extent of the actual contributing areas. This is the reason why *Wilson and Gallant* [2000] stated that the QDWI could not be used with multiple-flow-direction algorithms.

[14] The numerical method allows instead a fast computation of $a(d)$ patterns on the D∞ flow path pattern for durations up to the maximum time of concentration. The numerical method is much faster than the geometrical approach for durations above 1200 s (3 min to analyze the whole catchment for durations up to the catchments time of concentration). Unlike the geometrical method, the computational time using the numerical approach does not depend on the number of alternative flow paths generated by the flow-direction algorithm, but only on the spatial and temporal discretization adopted. With a computational time step

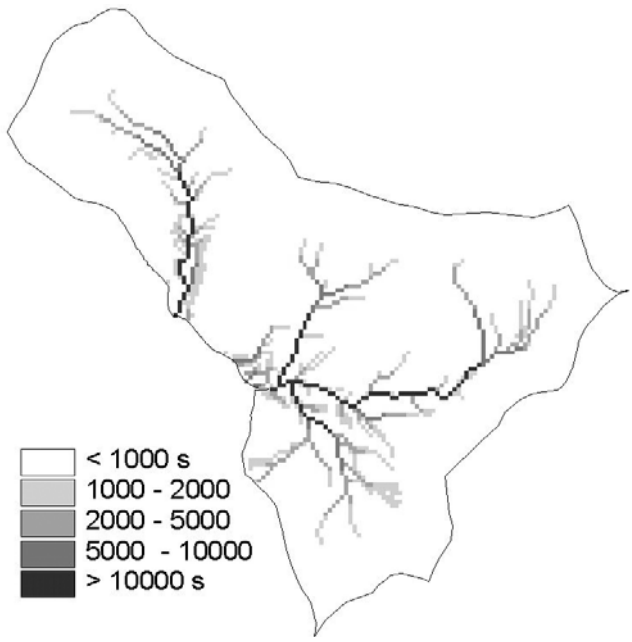

Figure 3. Map of the time of concentration computed with the geometrical approach on the D8 flow path pattern.

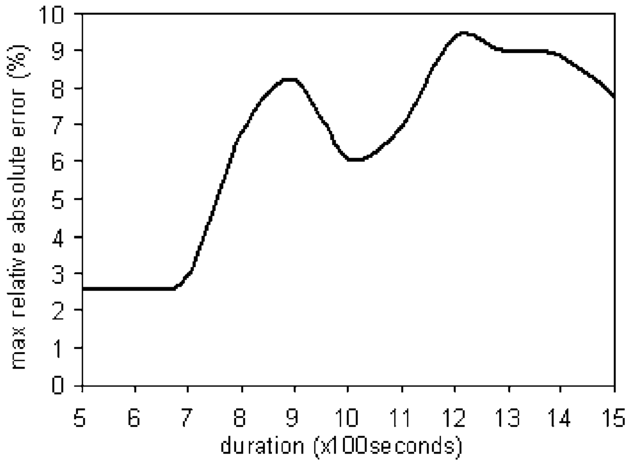

Figure 4. Maximum relative absolute error of the $a(d)$ patterns computed with the numerical approach compared with those computed with the geometrical approach, using the D∞ flow path pattern. Error is expressed as percentage of $a(d)$ computed with the geometrical approach.

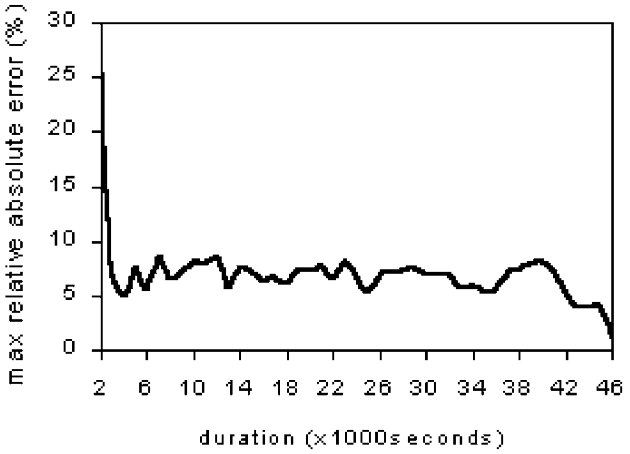

Figure 6. Maximum relative absolute error of the $a(d)$ patterns computed with the numerical approach compared with those computed with the geometrical approach, using the D8 flow path pattern. Error is expressed as percentage of $a(d)$ computed with the geometrical approach.

Δt = 2 s, corresponding to f $\cong$ 0.1 and 448,403 subelements, the results of the numerical and the geometrical methods for duration up to 1500 s differ by less than 10%. Figure 4 shows the maximum absolute relative errors, expressed as a percentage of $a(d)$ computed with the geometrical approach. Figure 5 shows a map of the absolute relative error for a duration of 1200 s, which is the duration with the largest errors.

[15] The performance of the numerical scheme for durations larger than 1500 s is evaluated by comparing the $a(d)$ patterns computed with the geometrical and the numerical methods on the D8 flow path pattern, for durations up to the maximum time of concentration (46,000 s). A computational time step Δt = 10 s, corresponding to $f \cong 0.5$ and a total number of subelements equal to 72,013, ensures numerical errors below 10% for durations larger than 2000 s. Figure 6 shows the maximum absolute relative errors, expressed as a percentage of $a(d)$ computed with the geometrical approach. Figure 7 shows a map of the absolute relative error for a duration of 2000 s, which is the duration with the largest errors. Errors above 10% occur in a few pixels located in areas of high convergence and with abrupt reductions in slope (i.e., celerity), for durations less than the upslope time of concentration. As for the case of D∞, the maximum numerical errors for durations less or equal to

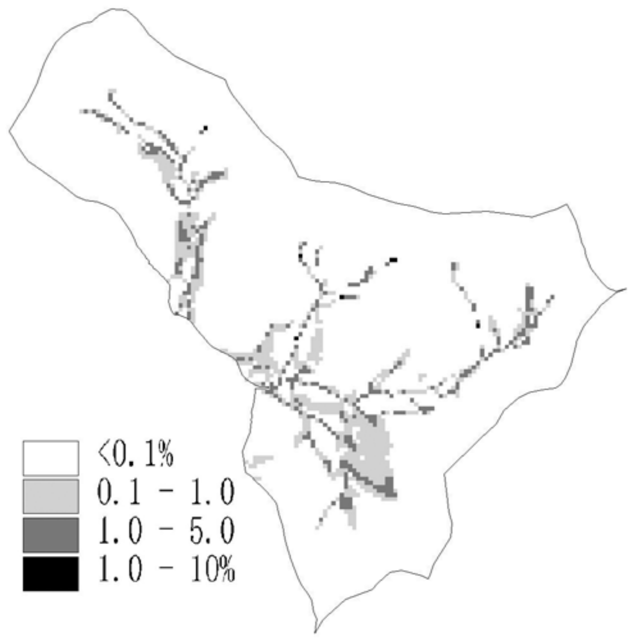

Figure 5. Map of the relative absolute difference between $a(d)$ computed on the D∞ flow path pattern with the numerical and the geometrical approach, for d = 1200 s.

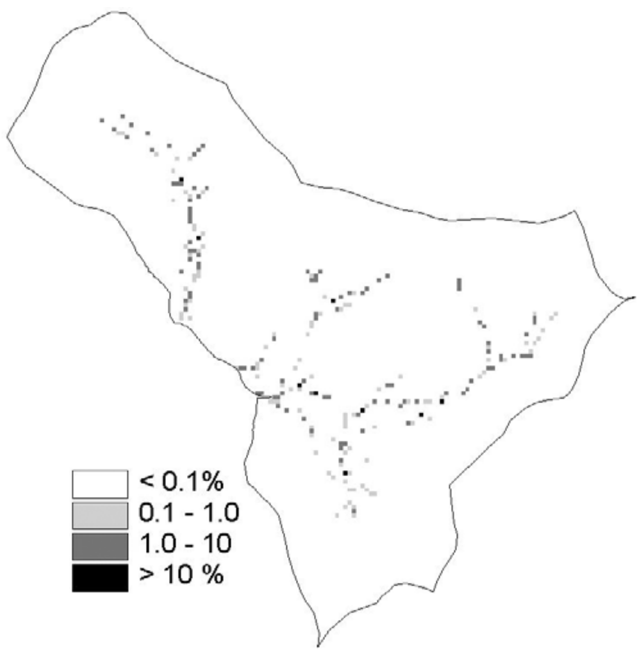

Figure 7. Map of the relative absolute difference between $a(d)$ computed on the D8 flow path pattern with the numerical and the geometrical approach, for = 2000 s.

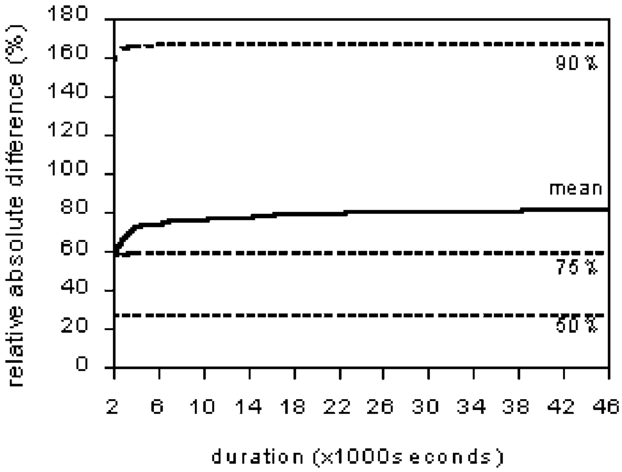

Figure 8. Relative absolute difference between $a(d)$ patterns computed with the numerical approach, using D8 and D∞ flow path patterns. The difference is expressed as a percentage of $a(d)$ computed using the D8 flow path pattern. The solid line is the average. The broken lines are the 50th, 75th, and 90th percentiles.

2000 s could be lowered to less than 10% by reducing the computational time step $\Delta t = 2$ s, corresponding to $f \cong 0.1$ and a total of 450,396 subelements.

[16] The structure of the lateral connectivity defined by the two flow-direction algorithms has a significant influence on the actual $a(d)$ patterns, since it affects the lateral distribution of the flow volumes. Figure 8 shows some statistics of the absolute differences between the $a(d)$ patterns computed with the numerical approach outlined above, using the D∞ and D8 flow path patterns. The absolute differences are expressed as a percentage of $a(d)$ computed using the D8 flow path pattern. The average value is about 70%, and approximately 25% and 165% at the 50th and the 90th percentiles, respectively, much larger differences than those between numerical and geometrical approaches. Given the documented superiority of the D∞ algorithm for flow path definition [*Tarboton*, 1997], it is clear that the numerical approach described in this technical note is a significant advancement for the computation of QDWI in practice.

5. Conclusions

[17] The quasi-dynamic wetness index (QDWI) can be an effective parametric approach for assessing the wetness conditions accounting for the timing of the lateral flow distribution [*Barling et al.*, 1994]. The established methodology for computing the QDWI is based on a geometrical analysis of the flow path length, and it is not practicable if grid-based multiple-flow-direction algorithms are to be used. The most recent studies based on the QDWI analysis were therefore forced to employ the D8 algorithm [e.g., *Borga et al.*, 2002; *Duan and Grant*, 2000; *Fried et al.*, 2000], despite this being recognized as inferior to multiple-flow-direction algorithms in tracking the flow path patterns [*Tarboton*, 1997]. In this technical note we present a numerical approach for computing the QDWI. The numerical method is just as accurate (at worst to within 10%) as the geometrical method and is capable of handling the large number of alternative upslope flow paths associated with multiple-flow-direction algorithms. Even with the relative errors associated with the numerical method, its computational efficiency and ability to work with multiple-flow-direction algorithms are superior to the geometrical approach, particularly when the QDWI analysis involves relatively large upslope areas with complex terrain.

[18] **Acknowledgments.** This work has been supported by the Cooperative Research Centre for Catchment Hydrology (Australia), the Australian Research Council (grants A39801842 and C39804872), and Österreichische Akademie der Wissenschaften (grant HÖ18). D∞ terrain analysis software is available online at http://www.engineering.usu.edu/dtarb. We also would like to thank the two anonymous reviewers and the associate editor whose thoughtful comments improved this manuscript.

References

Ambroise, B., K. J. Beven, and J. Freer, Toward a generalization of the TOPMODEL concepts: Topographic indices of hydrological similarity, *Water Resour. Res.*, *32*, 2135–2145, 1996.

Barling, R. D., I. D. Moore, and R. B. Grayson, A quasi-dynamic wetness index for characterizing the spatial distribution of zones of surface saturation and soil-water content, *Water Resour. Res.*, *30*, 1029–1044, 1994.

Beven, K. J., TOPMODEL: A critique, *Hydrol. Processes*, *11*, 1069–1086, 1997.

Beven, K. J., and J. Freer, A dynamic TOPMODEL, *Hydrol. Processes*, *15*, 1993–2011, 2001.

Beven, K. J., and M. J. Kirkby, A physically based, variable contributing area model of basin hydrology, *Hydrol. Sci. Bull.*, *24*, 43–69, 1979.

Beven, K. J., R. Lamb, P. Quinn, R. Romanowicz, and J. Freer, TOPMODEL, in *Computer Models of Watershed Hydrology*, edited by V. P. Singh, pp. 627–667, Water Resour. Publ., Highlands Ranch, Colo., 1995.

Borga, M., G. Dalla Fontana, and F. Cazorzi, Analysis of topographic and climatic control on rainfall-triggered shallow landsliding using a quasi-dynamic wetness index, *J. Hydrol.*, *268*, 56–71, 2002.

Chirico, G. B., R. B. Grayson, A. Longobardi, P. Villani, and A. W. Western, Shallow landlside hazard mapping based on a quasi-dynamic wetness index, in *MODSIM 2001: International Congress on Modelling and Simulation*, vol. 2, edited by F. Ghassemi et al., pp. 931–936, Modell. and Simulation Soc., Canberra, Australia, 2001.

Clark, C. O., Storage and the unit hydrograph, *Trans. Am. Soc. Civ. Eng.*, *110*, 1419–1488, 1945.

Duan, J., and G. E. Grant, Shallow landslide delineation for steep forest watersheds based on topographic attributes and probability analysis, in *Terrain Analysis: Principles and Applications*, edited by J. P. Wilson and J. C. Gallant, pp. 311–329, John Wiley, New York, 2000.

Fried, J. S., D. G. Brown, M. O. Zweifler, and M. A. Gold, Mapping contributing areas for storm water discharge to streams using terrain analysis, in *Terrain Analysis: Principles and Applications*, edited by J. P. Wilson and J. C. Gallant, pp. 183–204, John Wiley, New York, 2000.

Gallant, J. C., and J. P. Wilson, Primary topographic attributes, in *Terrain Analysis: Principles and Applications*, edited by J. P. Wilson and J. C. Gallant, pp. 51–85, John Wiley, New York, 2000.

Grayson, R. B., I. D. Moore, and T. A. McMahon, Physically based hydrologic modeling: 1. A terrain-based model for investigative purposes, *Water Resour. Res.*, *28*, 2639–2658, 1992.

Gritzner, M. L., W. A. Marcus, R. Aspinall, and S. G. Custer, Assessing landslide potential using GIS, soil wetness modeling and topographic attributes, Payette River, Idaho, *Geomorphology*, *37*, 149–165, 2001.

Jones, J. A. A., Some limitations to the a/s index for predicting basin-wide patterns of soil water drainage, *Z. Geomorphol.*, *60*, 7–20, 1986.

Moore, I. D., R. B. Grayson, and A. R. Ladson, Digital terrain modelling: A review of hydrological, geomorphological, and biological applications, *Hydrol. Processes*, *5*, 3–30, 1991.

O'Callaghan, J. F., and D. M. Mark, The extraction of drainage networks from digital elevation data, *Comput. Vision Graphics Image Processes*, *28*, 323–344, 1984.

O'Loughlin, E. M., Saturation regions in catchments and their relations to soil and topographic properties, *J. Hydrol.*, *53*, 229–246, 1981.

Piñol, J., K. J. Beven, and J. Freer, Modelling the hydrological response of Mediterranean catchments, Prades, Catalonia: The use of distributed models as aids to hypothesis formulation, *Hydrol. Processes*, *11*, 1287–1306, 1997.

Rossi, F., and P. Villani, Regional flood estimation methods, in *Coping With Flood*, edited by G. Rossi, N. Harmancioglu, and V. Yevjevich, pp. 135–170, Kluwer Acad., Norwell, Mass., 1994.

Schaake, J. C., J. C. Geyer, and J. W. Knapp, Experimental examination of the rational method, *J. Hydraul. Div. Am. Soc. Civ. Eng.*, *93*(6), 353–370, 1967.

Smith, A. A., A generalised approach to kinematic flood routing, *J. Hydrol.*, *45*, 71–89, 1980.

Smith, R. E., D. C. Goodrich, D. A. Woolhiser, and C. L. Unkrich, KINEROS: A KINematic runoff and EROSion model, in *Computer Models of Watershed Hydrology*, edited by V. P. Singh, pp. 697–732, Water Resour. Publ., Highlands Ranch, Colo., 1995.

Tarboton, D. G., A new method for the determination of flow directions and upslope areas in grid digital elevation models, *Water Resour. Res.*, *33*, 309–319, 1997.

Wilson, J. P., and J. C. Gallant, Secondary topographic attributes, in *Terrain Analysis: Principles and Applications*, edited by J. P. Wilson and J. C. Gallant, pp. 87–131, John Wiley, New York, 2000.

Woods, R. A., R. B. Grayson, A. W. Western, M. J. Duncan, D. J. Wilson, R. I. Young, R. P. Ibbitt, R. D. Henderson, and T. A. McMahon, Experimental design and initial results from the Mahurangi River Variability Experiment: MARVEX, in *Land Surface Hydrology, Meteorology, and Climate: Observations and Modeling*, *Water Sci. Appl. Ser.*, vol. 3, edited by V. Lakshmi, J. D. Albertson, and J. Shaake, pp. 201–213, AGU, Washington, D. C., 2001.

G. B. Chirico, Department of Agricultural Engineering, University of Naples Federico II, Via Università, 100, 80055, Portici, Italy. (gchirico@unina.it)

R. B. Grayson and A. W. Western, Centre for Environmental Applied Hydrology and Cooperative Research Centre for Catchment Hydrology, Department of Civil and Environmental Engineering, University of Melbourne, Victoria 3010, Australia.